Effects of Welding Parameters on Temperature Distribution and Tensile Strength of AA6061-T6 Welded by Friction Stir Welding

Dr. Majid Hameed Majeed
Assistant Professor
Middle Technical University
E-mail:drmajidhm@yahoo.com

ABSTRACT

The present research aims to study the effect of friction stir welding (FSW) parameters on temperature distribution and tensile strength of aluminum 6061-T6. Rotational and traverse speeds used were (500,1000,1400 rpm) and (14,40,112 mm/min) respectively. Results of mechanical tests showed that using 500rpm and 14mm/min speed give the best strength. A three-dimensional fully coupled thermal-stress finite element model via ANSYS software has been developed. The Rate dependent Johnson-Cook relation was utilized for elasto-plastic work deformations. Heat-transfer is formulated using a moving heat source, and later used the transient temperature outputs from the thermal analysis to determine equivalent stresses in the welded plates via a 3-D thermo- mechanical simulation. Motion due to rotation and translation of the tool induces asymmetry in the material flow and heating across the tool pin. The rotation speed results in stirring and mingling of material around the tool and the movable tool moves the stirred material from the front to the back of the tool and finishes welding process. Higher rotation speed rates create higher temperature because of higher friction heating and result in more powerful stirring and mingling of material. A good agreement is evident between experimental and Ansys results.

Key words: friction stir welding, aluminum 6061-t6, ansys, heat transfer, thermo-mechanical coupling , moving heating source, temperature distributions.

تاثير عوامل اللحام على توزيع درجات الحرارة ومقاومة الشد لسبيكة المينيوم 6061-T6 باستخدام لحام الاحتكاك الدوراني

د. ماجد حميد مجيد
استاذ مساعد
الجامعة التقنية الوسطى

الخلاصة

يهدف هذا البحث إلى دراسة العوامل المؤثرة على لحام الاحتكاك الدوراني (FSW) على توزيع درجة الحرارة وقوة الشد لمعدن الألومنيوم 6061-T6. حيث تم اختيار ثلاث سرع دورانية (500،1000،1400 دورة في الدقيقة) و وثلاث حركات خطية (التغذية) (14،40،112 ملم / دقيقة) على التوالي. وأظهرت نتائج الاختبارات الميكانيكية ان استخدام سرعة دورانية 500 دورة/الدقية وسرعة خطية 14ملم/ دقيقة تعطي أفضل قوة مقاومة للمعدن. وقد تم بناء أنموذج بلابعاد الثلاثة لتحليل الاجهادات الحرارية المزدوجة باستخدام برنامج ANSYS . حيث تم استخدام علاقة جونسون كوك لاخذ بنظر الاعتبار التشوهات المرنة-اللدنة . تم بناء انموذج لانتقال الحرارة باستخدام اسلوب مصدر حراري متنقل، حيث تم استخدام درجات الحرارة الناتجة كدالة للزمن واستخدامها لاحقا لحساب الاجهادات المكافئة في الالواح الملحومة من خلال انموذج ثلاثي الابعاد حراري-ميكانيكي. حيث تم الاخذ بنظر الاعتبار دوران وحركة الاداة التي تؤدي الى جريان المعدن وتوليد الحرارة عبر الاداة.

حيث تم دراسة النتائج بسرعة دوران في التحريك والمزج بين المواد حول الاداة و وحركة الاداة من الأمام إلى الخلف وانتهاء عملية اللحام. ارتفاع معدلات سرعة الدوران يؤدي الى مزج افضل بسبب تولد درجات حرارة عالية بسبب ارتفاع حرارة الاحتكاك لقد تم الحصول على تطابق جيد بالنتائج بين العملي والانسزز.
الكلمات الرئيسية : اللحام الاحتكاك الدوراني ، سبيكة المينيوم 6061-T6 , انسزز ، انتقال الحرارة، الازدواجية بين الميكانيك- الحرارة ، مصدر حراري متنقل، توزيع درجات الحرارة.

1. INTRODUCTION

The basic theory of FSW is outstanding simple. A non-consumable rotation tool with a specially shaped pin and shoulder is entered between two edges of sheets or plates, with abutting configuration, to be joined and travelled along the line of joint. The tool has two primary functions: (a) heating the work-piece, and (b) moving the material to produce the joint. The shoulder makes firm contact with the top surface of the work-piece. Heat generated by friction at the shoulder and to a lesser extent at the pin surface, softens the material being welded. Severe plastic deformation and flow of this plasticized metal occurs as the tool is translated along the welding direction. There have been widespread benefits resulting from the application of FSW in for example, aerospace, ship-building, automotive, and railway industries, **Esther, et al.,2006**, **Nadan, et al.,2008 and Mishra and Ma, 2005**. Tool traveling and rotation speeds, among other welding parameters, are most important variables that may affect the joint properties. In view of the literature survey and to the researcher knowledge, none has settle on an optimal value for these parameters as far as it concerned with FSW of A6061, but scattered values have been found. In **Soundararajan et al., 2005,** work tool travel and rotation speeds were (132, 330mm/min) and (344, 500 rpm). In **Somasekharan and Murr,2006**, work tool travel and rotation speeds were (90 mm/min) and (800 rpm) while in **Reddy et al., 2006**, work these parameters were (15 mm/min) and (800 rpm). The criterion used to define these parameters is that the values of tool traveling and rotation speeds which gives maximum tensile strength. **Yousif, 2006**, shown that specimen which contains FSW defects does not offer high tensile strength and elongation. In this work**,** two parameters are very acting in FSW: rotation speed rate **(**Spindle speed**,** rpm) and traverse speed rate (Feed rate, mm/min) along the line of joint are studied.

2. EXPERIMENTAL PART

2.1 Tool Geometry

Tool geometry designed and manufactured in this study is shown in **Fig.1**, which is a screw shoulder and cylindrical pin. The tool geometry plays a complicated role in material flow and in circuit controls the traverse rate at which FSW can be managed. FSW tool consists of a shoulder and a pin. The tool has two primary functions: (a) localized heating, and (b) material flow. In the initial stage of tool mixing, the heating produces at first from the friction between tool and work-piece. Some additional heating produces from deformity of material. The tool is soused until the shoulder touches the work-piece. The friction between the shoulder and work-piece results in the biggest former of heating. The shoulder also serves confinement for the heated measure of material. The second purpose of the tool is to 'stir' and 'move' the material. The tool's welding is manufactured from M2 tool steel and have a radius of shoulder (R_s=12.5mm) and pin radius (R_p=3mm).

2.2 Milling Machine

The vertical milling machine used in this research is shown in **Fig.2**, which is available in mechanical laboratory- Institute of Technology -Baghdad. The parameters used in this research is explained in **Table 1**. A special fixture was designed and manufactured to clamp the aluminum plates when welded to decrease the joint deformation. The butt joint configuration is

obtained by securing the welding samples into a carbon steel backing plate, the backing plate was fastened into the fixture and has been adjusted to have a level surface.

2.3 Chemical Test

Chemical test had been carried out in the Laboratories of the Institute of Technology – Baghdad. For aluminum plate before welding, results of the chemical tests are given in **Table 2**, it shows that the alloy is AA6061-T6.

2.4 Friction Stir Welding

Due to the lack of specialized stir welding machine, a vertical milling machine was used, the milling machine was operated with variable travelling and rotation speeds. The machine has been equipped by the researcher with tool, backing plate and fixture to be appropriate for FSW. Fixture and backing plate was machined from steel available tool steel alloy (AISI type S-5).

2.5 Tensile Test

In order to investigate mechanical properties of the work piece before and after welding process, a series of tensile tests had been performed to determine the yield strength, modulus of elasticity and elongation. **Fig.3** shows the specimen.

2.6 Temperature Measurement

Transient temperatures were recorder at three locations during FSW process using three gauges type thermocouples. The layout of the locations of the thermocouples are shown in **Fig.4**. One row of the thermocouples is placed in first, middle and end of the aluminum plates along the welding direction. The thermocouples in the row are placed at certain depth in plate, the first thermocouple is 1.5mm and the middle is 3mm and the third is 4.5mm from the top surface respectively. The location of thermocouples were at 13.5mm from the weld's centerline. These locations (three) were corresponding to the tool pin's edge. Drilling the holes from the bottom side of the plate, then beaded the thermocouples at the tip and the measuring points, with glue having highly thermal conductivity. The transient temperature from the thermocouples were recorded.

3. THEORETICAL PART

One of the key elements in the friction stir welding process is the generation of heat in the interface surface between the tool and the work-piece, this made the force to generate the FSW process successful. The temperature distribution varies with time and space, hence a three dimensional transient isotropic with moving heat source model was used to simulate FSW thermal process. The general heat transfer equation is:

$$\rho C_{p(T)} \frac{\partial T}{\partial t} = K_{(T)} \left(\frac{\partial^2 T}{\partial x^2} + \frac{\partial^2 T}{\partial y^2} + \frac{\partial^2 T}{\partial z^2} \right) + \dot{Q} \quad (1)$$

The boundary conditions in the FSW was the energy loss by heat convection ,**Nandan, et al., 2006**. as in the following equation:

$$Q_{conv.} = h(T - T_{\infty}) \quad (2)$$

And convection coefficient for the work-piece / backing plate (Q_{back}) is calculated as in the following equation ,**Soundararajan et al., 2005 and Nandan et al., 2007**.

$$Q_{back} = h_b(T - T_\infty) \quad (3)$$

And another boundary condition was the radiation heat loss by the following equation:

$$Q_{rad} = eF\sigma_{SB}(T^4 - T_\infty^4) \quad (4)$$

Heat generation during friction stir welding arises from two main sources, the first one is the deformation of the material around the tool, and the second is the friction at the surface of the tool , **Sarmad, 2010**. Frictional heat for the shaft rotating at rubbing angular speed of $(1-\delta)\omega$ is : $dQ_s = (1-\delta)\ \omega\ dM$
where the torque $dM = \mu pr\ dA = 2\pi\mu pr^2\ dr$

hence $dQ_s = 2\pi\mu(1-\delta)\ \omega\ p\ r^2\ dr$ (5)

where δ is between 0.6 and 0.85 ,**Nandan et al., 2007 and Hani et al., 2013**. Hence, the total frictional heat of shoulder will be;

$$Q_s = \int_0^R dQ_s = \frac{2}{3}\pi(1-\delta)\ \omega\ \mu\ p\ R_s^3 \quad (6)$$

Similar concept, heat generated by lateral surface of the pin is:

$$Q_p = 2\pi(1-\delta)\omega\ \mu\ p\ L_p\ R_p^2 \quad (7)$$

The total heat generation is :

$$Q_T = 2\pi(1-\delta)\omega\ \mu\ p\ \left(\frac{R_s^3}{3} + L_p\ R_p^2\right) \quad (8)$$

The empirical equation for calculating the heat input to the work-piece is given by **Chao and Qi, 1998**.

$$q_{(r)} = \frac{3\ Q\ r}{2\ \pi\ (r_s^3 - r_p^3)} \quad \text{for } r_p \le r \le r_s \quad (9)$$

The total heat input to the work-piece:

$$Q = \frac{\pi\ \omega\ \mu\ F\ (R_s^2 + R_s R_p + R_p^2)}{45(R_s + R_p)} \quad (10)$$

The frictional heating in the thin layer near the interface was treated as a surface heat generation term q . , **Feng et al., 2007**.

$$q = \frac{2\ \eta\ \mu\ F\ \omega}{60(R_s^2 + R_p^2)}\ r \qquad \text{for } r_p < r < r_s \quad (11)$$

A wide range of published values for friction coefficient (μ) is within (0.3-0.85) ,**Dixon et al., 2007**. Convection and radiative heat losses to the ambient occurs across all free surface of the work-piece and conduction losses occur from the work-piece bottom surface to the backing

plate. The proposed model account only for frictional heat generated at shoulder and pin surface instead of modeling heat generated by plastic deformation.

4. ANSYS SIMULATION OF THE FSW

To simulate the friction stir welding (FSW) process. Several characteristics of FSW are presented, including tool-workpiece surface interaction, heat generation due to friction, and plastic deformation. A nonlinear direct coupled-field analysis is performed, as thermal and mechanical behaviors are mutually dependent and coupled together during the FSW process. A cylindrical rotating tool plunges into a rigidly clamped workpiece and moves along the joint to be welded. As the tool moved along the joint, the generation of heat through friction between the tool shoulder and the workpiece. Additional heat is generated by plastic deformation of the workpiece material. The generated heat results in thermal softening of the workpiece material. The model consists of a coupled-field solid element with structural and thermal degrees of freedom. The temperature rises at the contact interface due to frictional contact between the tool and workpiece. The simulation welds two 6061-T6 aluminum plates (workpiece) with a cylindrical shape tool, as shown in **Fig.5**. Two rectangular shaped plates are used as the workpiece. The plate size is (330x184x6.5 mm). The tool shoulder diameter is (25 mm). Both the workpiece (Aluminum plates) and the tool are modeled using coupled-field element SOLID226 with the structural-thermal option (KEYOPT(1) =11). Surface-to-surface contact pair TARGE170 and CONTA174 is used. To simulate a perfect thermal contact between the plates, a high thermal contact conductance (TCC) of $2x10^6$ W/m^2 °C is specified. The tool plunges into the work piece, rotates, and moves along the weld line. Because the frictional contact between the tool and workpiece is primarily responsible for heat generation, a standard surface to-surface contact pair is defined between the tool and workpiece ,**Ansys, help,2014**. The CONTA174 element is used to model the contact surface on the top surface of the workpiece, and the TARGE170 element is used for the tool. A low TCC value (10 W/m^2 °C) is specified for this contact pair because most of the heat generated transfers to the workpiece. The coefficient of friction (0.4 to 0.2) is defined (TB,FRIC with TBTEMP and TBDATA). A multipoint constraint (MPC) algorithm with contact surface behavior defined as bonded always is used to constrain the contact nodes to the rigid body motion defined by the pilot node. Thermal properties of the AA6061-T6 plates , **Prasanna, et al., 2010 and Zhu and Chao, 2004**. such as thermal conductivity, specific heat, and density and Mechanical properties of the plates such as Young's modulus and the coefficient of thermal expansion are temperature-dependent shown in **Table 3**. To simulate the material of the workpieces in the analysis, using a temperature and strain rate dependence law of material was used using the elastic-plastic Johnson-Cook material model , **Johnson and Cook, 1983**. which is given by:

$$\sigma_y = [A + B(\bar{\varepsilon}^{pl})^n]\left[1 + Cln\frac{\dot{\bar{\varepsilon}}^{pl}}{\dot{\varepsilon_o}}\right]\left[1 - \left(\frac{T - T_{ref}}{T_{melt} - T_{ref}}\right)^m\right] \quad (12)$$

where σ_y is the yield stress, $\bar{\varepsilon}^{pl}$ is the effective plastic strain, $\dot{\bar{\varepsilon}}^{pl}$ is the effective plastic strain rate, ε_o is the normalizing strain rate (typically, 1.0 /s). *A, B, C, n, T_{melt},* and *m* are material constants, which are listed in **Table 4**. T_{ref} is the temperature of ambient, that is 22 °C in this case. The model of material was plasticity's model with the law of hardening and dependent rate. **Fig.6** shows stress strain curves for Johnson-Cook hardening at various temperatures.

Thermal and mechanical boundary conditions imposed on the FSW model. The workpiece is fixed by clamping each plate , **Zhu and Chao, 2004**. The clamped portions of the plates are constrained in all directions. The loading represented by rotating tool moves along the weld line.

The tool plunges into the workpiece at a very shallow depth, then rotates to generate heat. The depth and rotating speeds are the critical parameters for the weld temperatures. Three cases are studies in this paper according to the changing the parameters as in **Table 1**. Spindle speed and the feed rate. A nonlinear transient analysis is performed using structural-thermal options of SOLID226 and CONTA174.

5- RESULTS AND DISCUSSION

5.1 Stress-Strain Diagrams

Fig.7 shows the three welding aluminum plates by FSW with different spindle speed and feed rate mention **in Table 1** . From each resulted plate, two tensile specimens are cut, one at the start of the plate and the other at the end of the plate as shown in **Fig.8**. The result's stress – strain diagrams shown in **Fig.9**.

5.2 Temperature Distribution

Tool design influences heat generation, plastic flow, the power required and the uniformity of the welded joint. The shoulder generates most of the heat, while both the shoulder and the tool pin affect the material flow. Motion due to rotation and translation of the tool induces asymmetry in the material flow and heating across the tool pin. The rotation speed results in stirring and mingling of material around the tool and the movable tool moves the stirred material from the front to the back of the tool and finishes welding process. Higher rotation speed rates create higher temperature because of higher friction heating and result in more powerful stirring and mingling of material. However, it should be noted that friction between the tool surface and work-piece is going to govern the heating. The calculated frictional heat generation and plastic heat generation show that the friction between the tool shoulder and workpiece is responsible for generating most of the heat. Heat-transfer is formulated using a moving heat source, and later used the transient temperature outputs from the thermal analysis to determine equivalent stresses in the welded plates via a 3-D thermo-mechanical simulation. **Table 5** shows the results of FSW in using the three parameters study were (500,1000,1400 rpm) and (14,40,112 mm/min) respectively and tensile strength for each case also the elongation in each case.

Results of mechanical tests showed that using 500rpm and 14mm/min speed give the best strength, hence **Fig.10** shows the temperature distribution in case of (500rpm and feed 14mm/min) and **Fig.11** shows the stress distribution in this case. **Figs**. **12 and 13** show plastic heat rate against time and frictional heat rate against time respectively. **Fig.14** shows resulting temperature profile as taken from experiment and ANSYS, for the purpose of comparison, it can be observed that the peak temperature resulting from transient thermal analysis is more than experimental results since the lake of accuracy in modeling of heat transfer. In actual case heat transfer through the fixture will increase the cooling process of the workpiece.

6. CONCLUSIONS

The results of temperature distribution and stresses are significantly changed with changing the rotational and traverse speeds used (500,1000,1400 rpm) and (14,40,112 mm/min) respectively. These parameters affect the temperature values and distribution. Results of mechanical tests showed that using 500rpm and 14mm/min speed give the best strength. A three dimensional heat transfer model was successfully developed to predict the temperature at different parameter. It can be observed that heat generated from the friction is approximately 90% transferred to the workpiece. A good agreement is evident between the experimental and Ansys results.

REFERENCES

- ASTM, 2005, *Standard Test Methods for Tension of Metallic Materials* [Metric] ASTM standard, Volume 03.01, Section 03.
- Adibi-Sedeh, A., Madhavan, V., and Bahr, B., 2003, *Extension of Oxley's Analysis of Machining to Use Different Material Models*, Transactions of the ASME, PP. 656-666.
- Aluminum Association, MATTER project, 2001.
- Ansys V.15 help, 2014, Ansys Elements Reference.
- Chao, Y., and Qi, X., 1998, *Thermal and Thermo-Mechanical Modeling of Friction Stir Welding of Aluminum Alloy 6061-T6*, Journal of Materials Processing & Manufacturing Science, vol. 7, PP. 215-233.
- Dixon, John, Burkes, Douglas and Medreder, Pavel, 2007, *Thermal Modeling of a Friction Bonding Process*, Proceeding Of COMSOL conference, Boston.
- Esther T. Akinlabi and Stephen A. Akinlabi, 2006, *Friction Stir Welding Process: A* green Technology. International Journal of Mechanical, Industrial Science and Engineering. Vol. 6, PP. 1489-1491.
- Feng, Z., Wang, X.L. David, S.A. and Sklad , P.S., 2007, *Modeling of Residual Stresses and Property Distributions in Friction Stir Welds of Aluminum 6061-T6*, Science and Technology of welding and joining , 12 (4), PP. 348-356.
- Hani Aziz Ameen, Ahmed Hadi Abood and Nabeel Shallal Thamer, 2013, *Theoretical and Experimental Investigation of Friction Stir Welding for Copper Alloy* , Al-Qadisiya J. for Eng. Sci., Vol.6, No.3, PP. 332-351.
- Johnson, G., and Cook, W., 1983, *A Constitutive Model and Data for Metals Subjected to Large Strains, High Strain Rates and High Temperatures*, Proceeding of the 7th Int. Symp. On Ballistics, The Hague, the Netherlands, PP. 1-7.
- Mishra R. S. and Z. Y. Ma., 2005, *Friction Stir Welding And Process*. Material Science and Engineering. Vol. 50, PP. 1-78.
- Mokhtar Awang, 2007, *Simulation of Friction Stir Spot Welding (FSSW) Process: Study of Friction Phenomena*, Ph.D. thesis, Virginia University.
- Nadan R., T. DebRoy and H. D. Bhadashia, 2008, *Resent Advanced ni Friction Stir Welding -Process, Weldment Structure and Properties*. Material Science. Vol.53, PP. 980-1023.
- Nandan, R., Prabu, B., De, A. and Debroy T., 2007, *Improving Reliability oh Heat Transfer and Materials Flow Calculations During Friction Stir Welding of Dissimilar Aluminum Alloys* , welding J., Vol. 86, PP. 313-322.

- Nandan, R., Roy G.G. and Debroy, T., 2006, *Numerical Simulation of Three Dimensional Heat Transfer and Plastic Flow During Friction Stir Welding,* Metallurgical and Materials Transactiona, A, Vol. 37 A , PP. 1247-1269.

- Nandan, R., Roy, G.G., Lienert, T.J. and Debroy, T., 2007, *Three Dimensional Heat and Material Flow During Friction Stir Welding of Mild Steel,* Acta Materialia, No.55, PP. 883-895.

- Prasanna, P., B. S. Rao, and G. K. Rao., 2010, *Finite Element Modeling for Maximum Temperature in Friction Stir Welding and its Validation Journal of Advanced Manufacturing Technology*. 51, PP. 925-933.

- Reddy, G. Madhusudhan, Mastanaiah, P., Murthy, C.V.S., Mohandas, T. and Viswanathan, N., 2006, *Microstructure, Residual Stress Distribution and Mechanical Properties of Friction- Stir AA6061 Aluminum Alloy Weldments* Proc. National seminar on non-destructive evaluation , Dec.7-9, Hydarabad.

- Sarmad Dhia Ridha, 2010, *Theoretical and Experimental Study For Measurement of Residual Stresses Induced by Friction Stir Welding and Investigation of Stress Relieve by Vibration in Aluminum Alloy,* Ph.D. thesis, Baghdad University.

- Somasekharan, A.C. and Murr, A.L.E., 2006, *Characterization of Complex, Solid-State Flow and Mixing in the Friction-Stir Welding of Aluminum Alloy 6061-T6 To Magnesium Alloy AZ91D Using Color Metallography*". J. Mater. Sci. No5370.

- PP. 5365-Sound dvarajan, Vijay, Zekovic, Srdja and Kovacevic, Radovan, 2005, *Thermo-Mechanical Model with Adaptive Boundary Conditions for Friction Stir Welding of AL6061,* International J. of Machine Tools and manufacture, Vol. 45, PP.1577-1587.

- Yousif, Mohanned Akab, 2006, *Investigation of Mechanical and Microstructural Characteristic of Friction Stir Welded Joints,* Ph.D. thesis, University of Baghdad.

- Zhu, X. K., and Y. J. Chao, 2004, *Numerical Simulation of Transient Temperature and Residual Stresses in Friction Stir Welding of 304L Stainless Steel,* Journal of Materials Processing Technology. 146.2, PP. 263-272.

NOMENCLATURE

$Cp_{(T)}$	temperature dependent of specific heat of work-piece, J/Kg°C
e	emissivity of radiant surface (e=0.5)
F	radiation view factor (F=1)
$K_{(T)}$	temp. dependent thermal conductivity coefficient of the work-piece, W/m°C
$\dot{Q}$	rate of heat generation , W
$Q_{conv.}$	energy loss by convection per unit area ,W
Q_{back}	energy loss of by convection per unit area, W
Q_{rad}	energy loss of by radiation by unit area, W
Q_{rad}	energy loss of by radiation by unit area, W
Q_s	heat generation by shoulder, W
Q_p	heat generation by pin , W

T	temperature, °C, K
t	time, sec
h, h_b	convection heat transfer coefficient, W/m^2°C
T_∞ , T_{ref}	absolute ambient temperature, °C, K
L_p	pin length , mm
R_s	shoulder radius, mm
R_p	pin radius , mm
p	interfacial pressure, Pa
S	spindle speed , rpm
R	feed rate , mm/min
σ_y	yield stress, Pa
ε^{pl}	effective plastic strain
$\dot{\varepsilon}^{pl}$	effective plastic strain rate
ε_o	normalizing strain rate
ρ	density of work-piece, Kg/m^3
σ_{SB}	s-Boltzman constant ($\sigma_{SB} = 5.67x10^{-8}\ W/m^2K^4$)
δ	slip factor that compensate for tool (material relative velocity)
ω	tool rotational speed, rpm
η	process efficiency

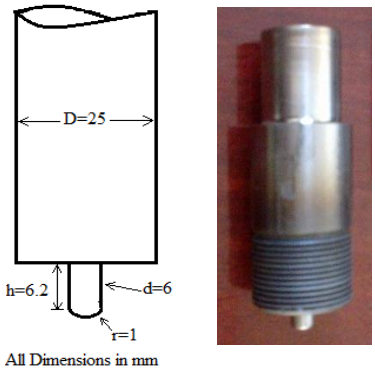

Figure 1. Screw shoulder and cylindrical pin.

Figure 2. Milling machine.

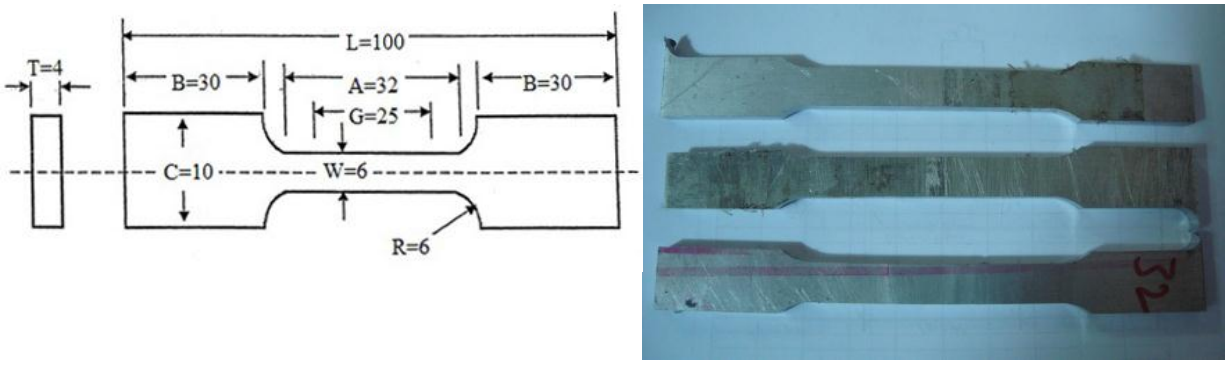

Figure 3. Rectangular tension test specimen ,**ASTM,2005**.

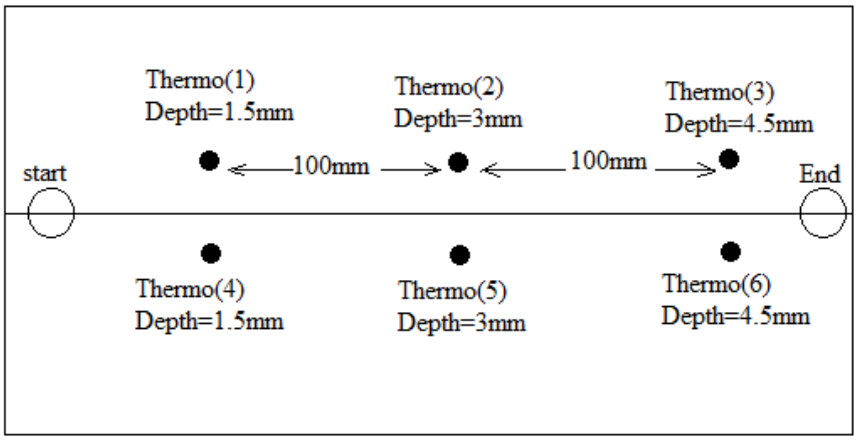

Figure 4. Layout of the locations of the thermocouples.

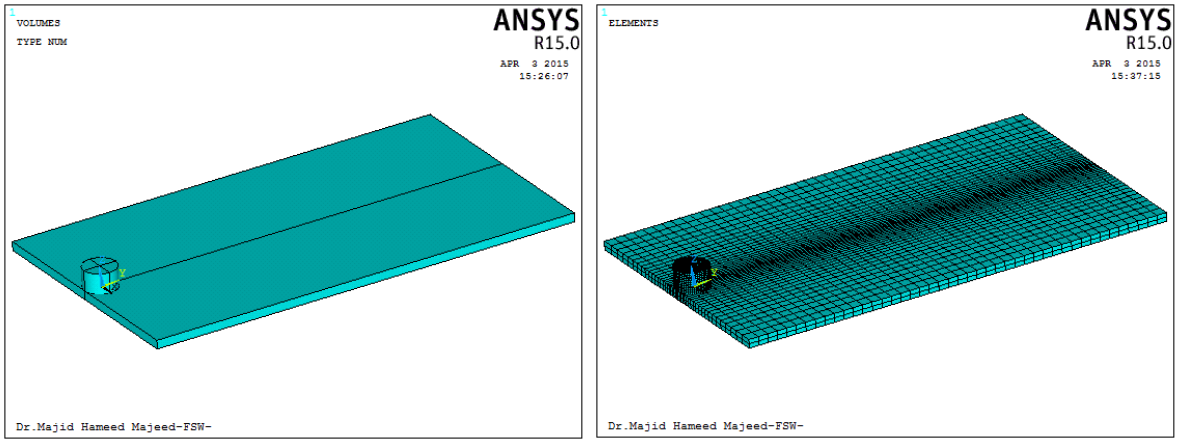

Figure 5. 3-D Model of workpiece and tool with finer mesh.

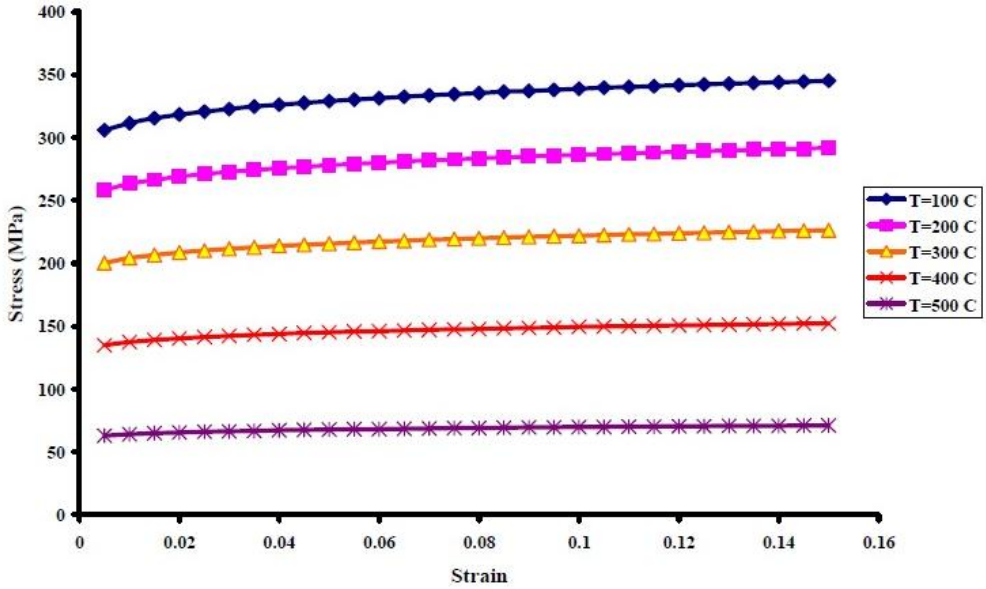

Figure 6. Plot of stress strain curve for Johnson-Cook work hardening ,**Mokhtar,2007**.

S=1000 rpm,R=40mm/min S=1400 rpm,R=112mm/min S=500 rpm,R=14mm/min

Figure7. Aluminum welding plate with different condition.

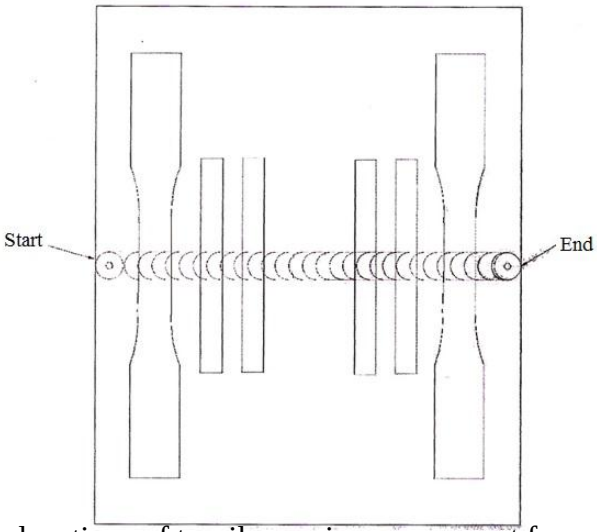

Figure 8. The locations of tensile specimens were cut from the weld plates.

Start	End

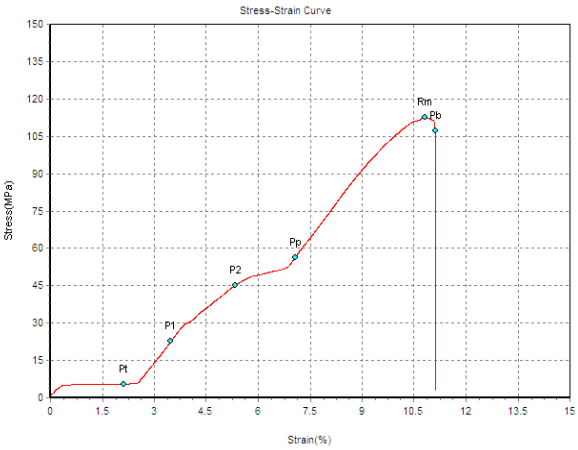

S=1000 rpm, R=40mm/min

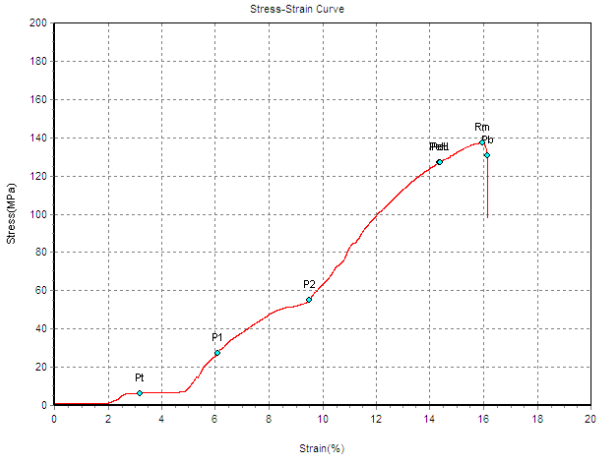

S=1000 rpm, R=40mm/min

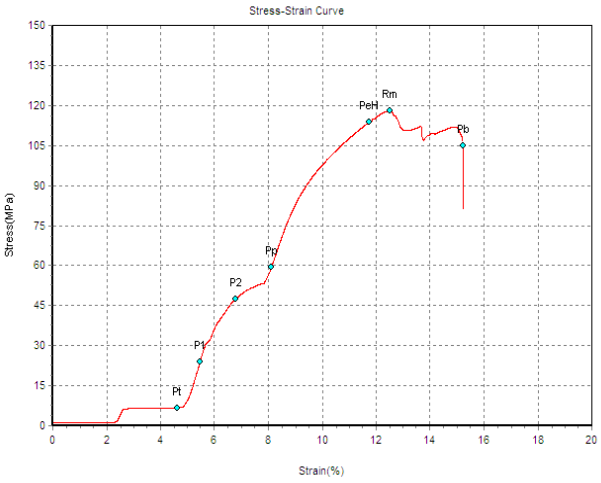

S=1400 rpm, R=112mm/min

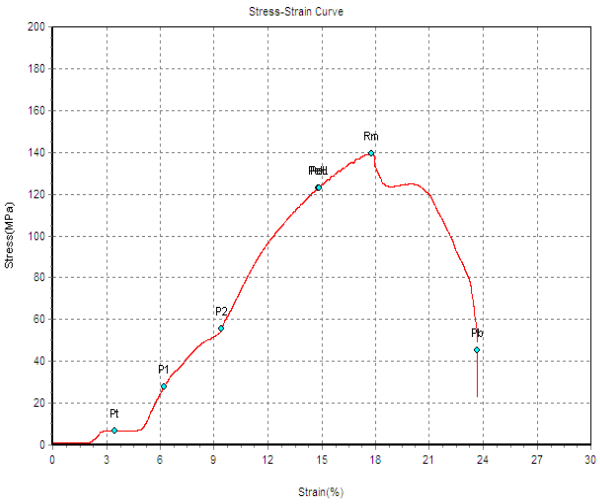

S=1400 rpm, R=112mm/min

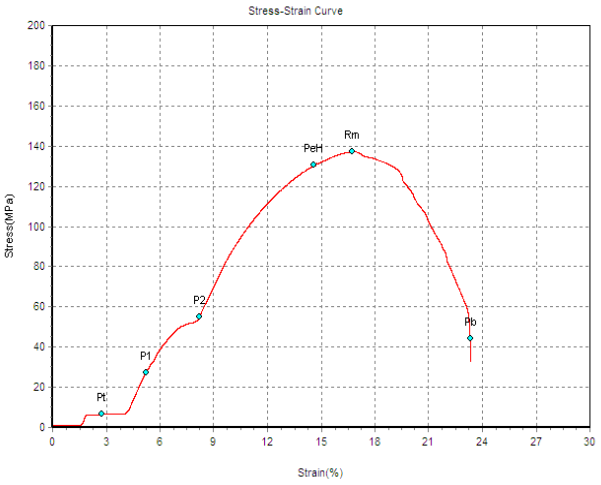

S=500 rpm, R=14mm/min

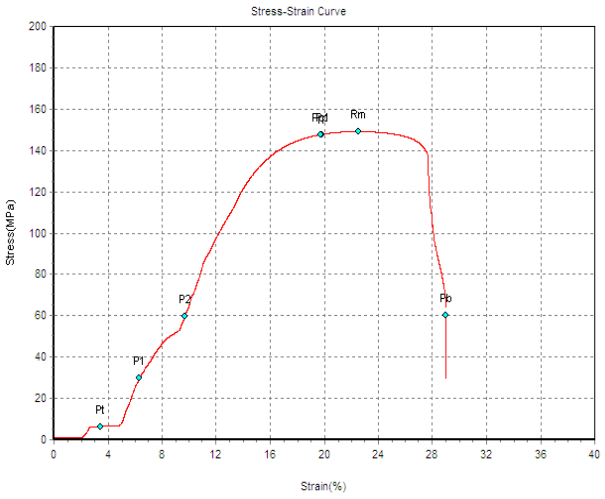

S=500 rpm, R=14mm/min

Figure 9. Stress-Strain diagrams for different parameters.

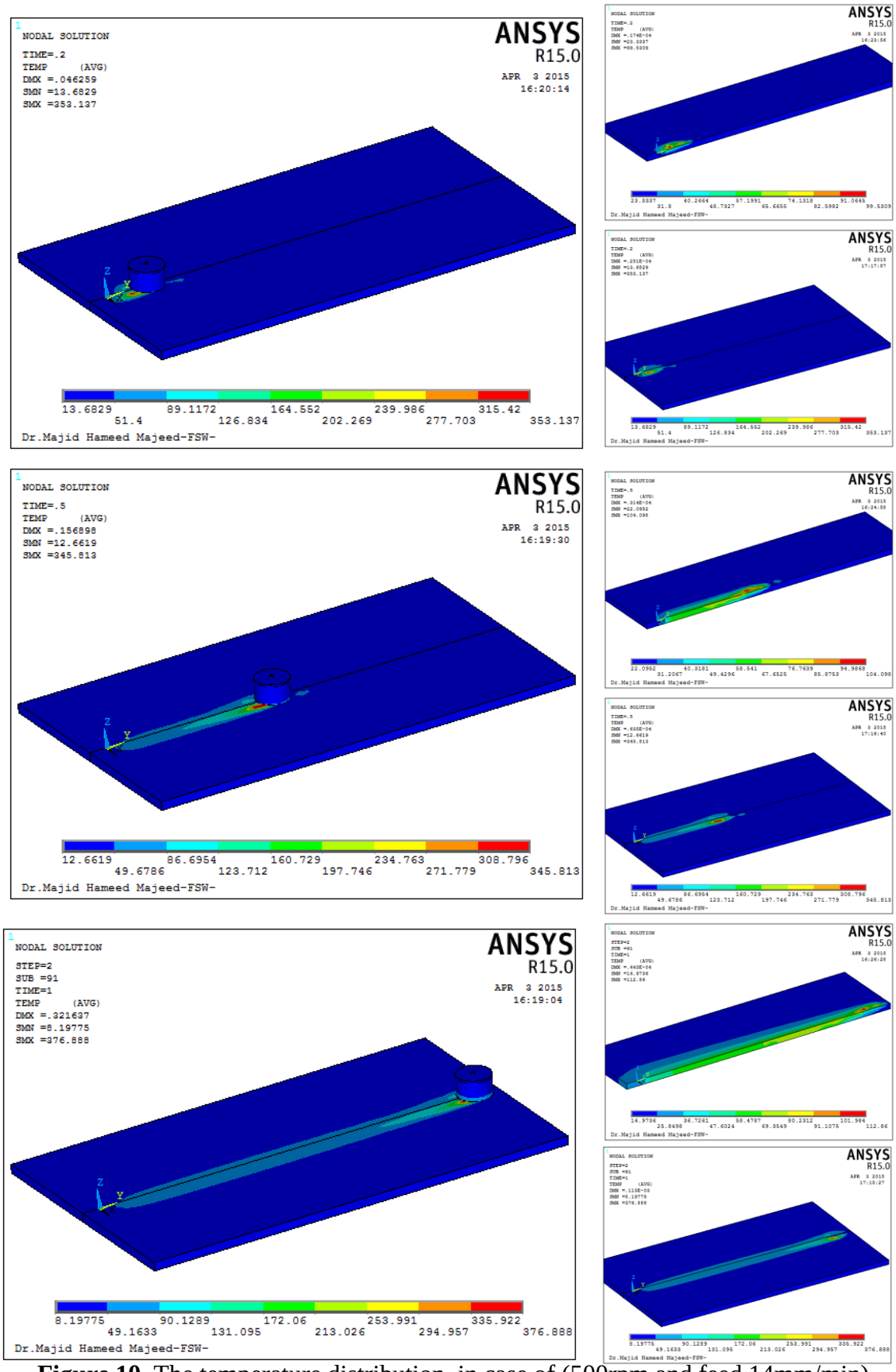

Figure 10. The temperature distribution in case of (500rpm and feed 14mm/min) .

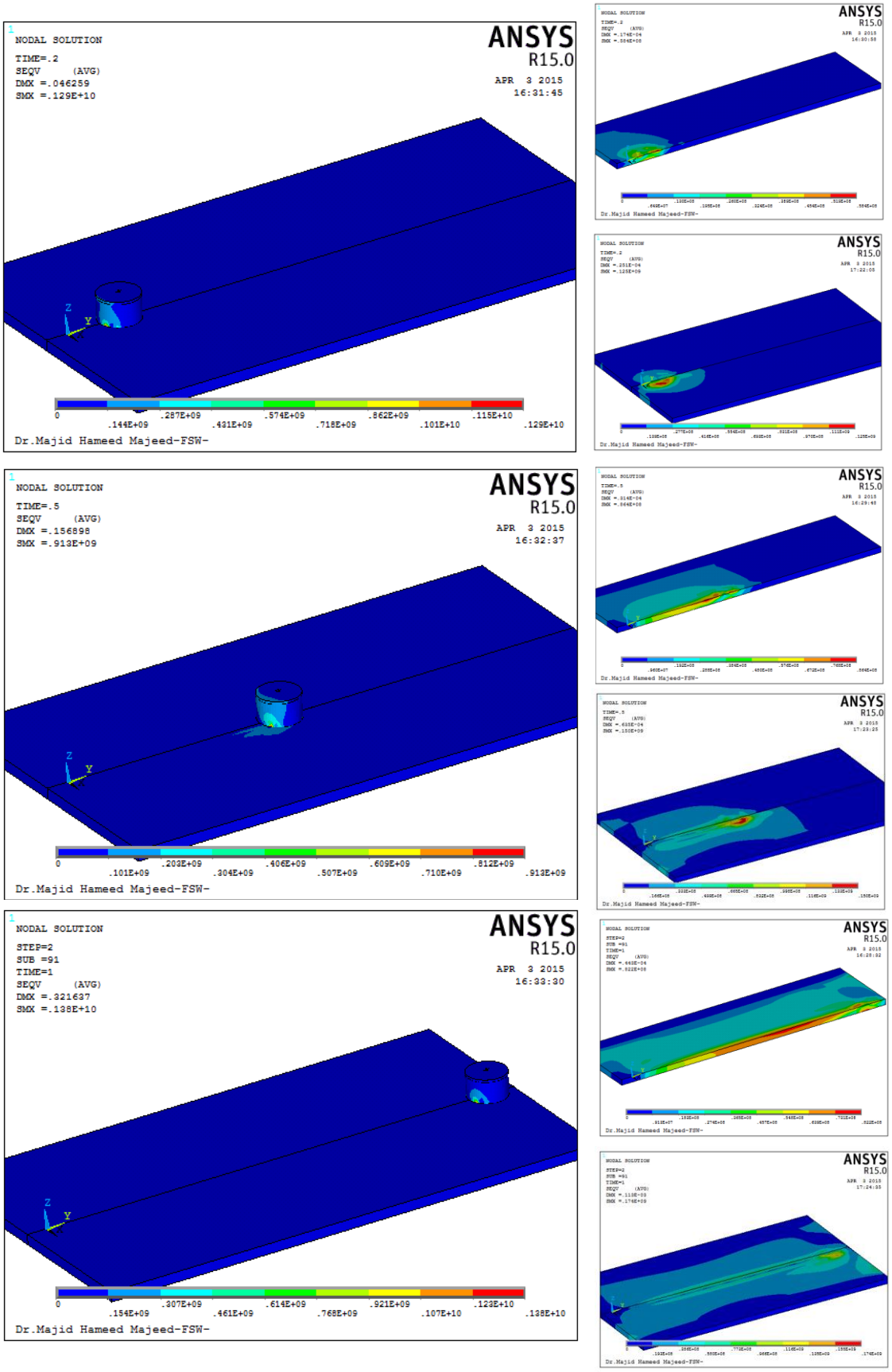

Figure 11. The stress distribution in case of (500rpm and feed 14mm/min).

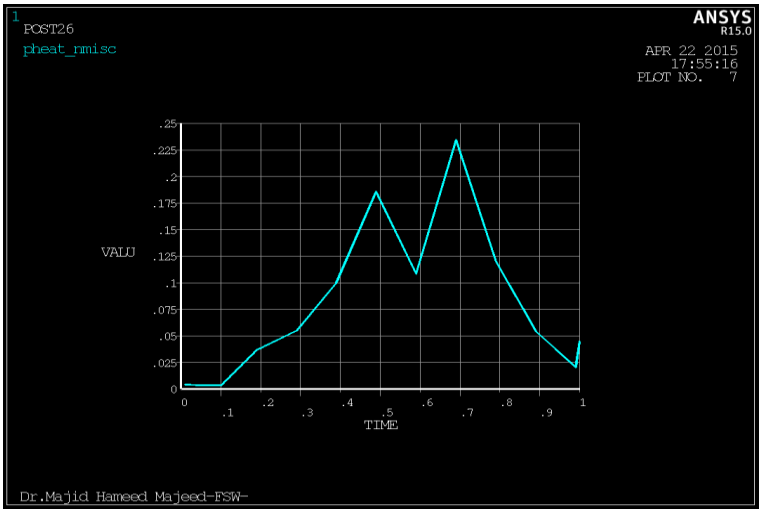

Figure 12. Plastic heat rate against time for 500rpm and feed 14mm/min.

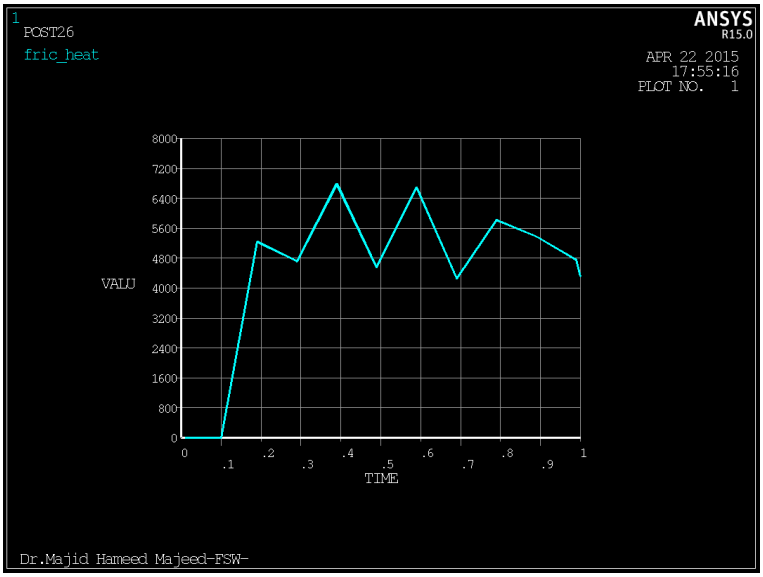

Figure 13. Frictional heat rate against time for 500rpm and feed 14mm/min.

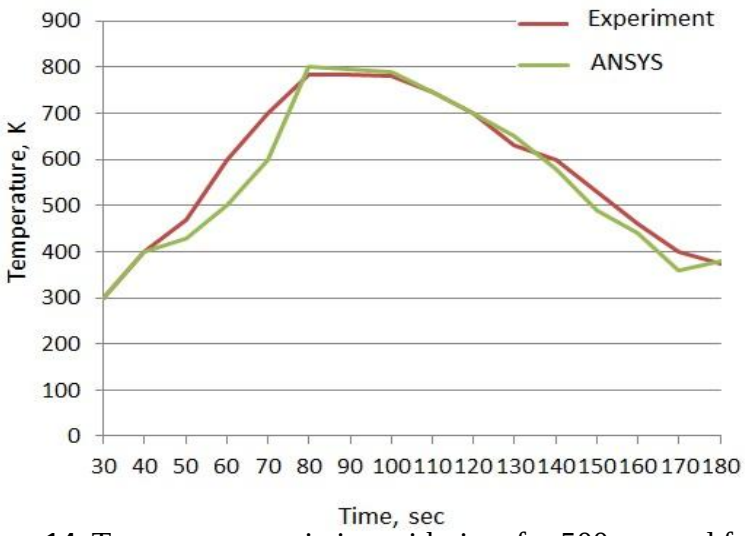

Figure 14. Temperature variation with time for 500rpm and feed 14mm/min.

Table 1. Parameters studied.

Spindle speed (S) (rpm)	1000	500	1400
Feed rate (R) (mm/min)	40	14	112

Table 2. Chemical compositions.

	Si	Fe	Cu	Mn	AL	Mg	Cr	Ni	Zn	Ti
Standard [**Al,2001**]	0.4-0.8	0-0.7	0.15-0.4	0-0.15	Bal.	0.8-1.2	0.04-0.35	0-0.15	0-0.15	0-0.15
Present Work	0.621	0.529	0.299	0.0852	Bal.	1.03	0.198	0.0096	0.0594	0.018

Table 3. Temperature dependent material properties for Aluminum alloy 6061-T6 ,**Chao and Qi,1998**.

Temperature	°C	37.8	93.3	148.9	204.4	260	315.6	371.1	426.7
Thermal Cond.	W/m°C	162	177	184	192	201	207	217	223
Heat Capacity	J/Kg°C	945	978	1004	1028	1052	1078	1104	1133
Density	Kg/m^3	2685	2685	2667	2657	2657	2630	2630	2602
Young's Modulus	GPa	68.54	66.19	63.09	59.16	53.99	47.48	40.34	31.72
Yield strength	MPa	274.4	264.6	248.2	218.6	159.7	66.2	34.5	17.9
Thermal Exp.	10^{-6}/°C	23.45	24.61	25.67	26.60	27.56	28.53	29.57	30.71

Table 4. Constants for Johnson- Cook material model ,**Adibi et al., 2003**.

Material	T_{melt} (°C)	A (MPa)	B (MPa)	C	n	m
AA 6061-T6	582	293.4	121.26	0.002	0.23	1.34

Table 5. The results of FSW.

No.	**Material**	**Specimen No.**	**Temp. at 1.5mm depth °C**	**Temp. at 3mm depth °C**	**Temp. at 4.5mm depth °C**	**Spindle speed rpm**	**Feed rate mm/min**	**Tensile test number (1)**	**Tensile test number (2)**	**Thickness of plate mm**	**Elongation % (1)**	**Elongation % (2)**
1	6061-T6	1	408	419	435	1000	40	113MPa (Start)	137MPa (End)	6.5	11	16
2	6061-T6	2	189	182	258	500	14	137MPa (Start)	149MPa (End)	6.5	23.5	29
3	6061-T6	3	282	228	315	1400	112	118MPa (Start)	134MPa (End)	6.5	15	23.5